# Nuclear quadrupole moment determination of $^{35}$Cl, $^{79}$Br, and $^{127}$I

R. E. Alonso
*Departamento de Física de Cs. Exactas, Universidad Nacional de La Plata, CC67, Caixa Postal 1900 La Plata, Argentina*

A. Svane
*Institute of Physics and Astronomy, University of Aarhus, DK-8000 Aarhus C, Denmark*

C. O. Rodríguez
*IFLYSIB, Grupo de Física del Sólido, CC565, Caixa Postal 1900 La Plata, Argentina*

N. E. Christensen
*Institute of Physics and Astronomy, University of Aarhus, DK-8000 Aarhus C, Denmark*

(Received 18 September 2003; revised manuscript received 3 December 2003; published 10 March 2004)

The electric-field gradient at the halide site is calculated in several compounds of Cl, Br, and I. The *ab initio* full-potential linear-augmented plane-wave method is employed with the generalized gradient approximation for exchange and correlation effects. The nuclear quadrupole moments of $^{35}$Cl, $^{79}$Br, and $^{127}$I are obtained by comparison of available experimental nuclear quadrupolar resonance data to the calculated electric-field gradients. The values of $|Q(^{35}\mathrm{Cl})| = 0.0855$ b, $|Q(^{79}\mathrm{Br})| = 0.330$ b, and $|Q(^{127}\mathrm{I})| = 0.721$ b are derived with $\sim 3\%$ statistical uncertainty. These values are in agreement with recent values derived by other methods, and thus confirm the validity of the present methodology for the determination of electric-field gradients in solids.

DOI: 10.1103/PhysRevB.69.125101 PACS number(s): 76.60.Gv, 76.80.+y, 21.10.Ky, 71.20.Ps

## I. INTRODUCTION

Several nuclear experimental techniques including nuclear magnetic resonance,[1] nuclear quadrupolar resonance (NQR),[2] time differential perturbed angular correlations (TDPAC),[3] Mössbauer spectroscopy,[4,5] and also electron paramagnetic resonance[6] (EPR) are widely utilized for the study of the properties of solids through the determination of the electric-field gradient (EFG) tensor at the position of the nucleus. These techniques exploit specific nuclear characteristics (distinct isotopes, decay of excited nuclear states, nuclear spin transitions, etc.), which involve the coupling between the nuclear quadrupole moment and the EFG. In some cases, the probe nuclei belong to the compound constituents, in other cases they are dopants introduced into the host. For example, in TDPAC the impurity concentration can be as low as a few ppm. The above techniques have been in use for several decades, and are of considerable importance for the study of solid-state systems, due to the fact that the EFG is a microscopic quantity providing information about the local environment of the nuclear probe. In addition, these techniques are mainly noninvasive, except for the cases of the impurity probe and possible radiation damage following implantation and/or decay.

Although the main interest is usually centered on the variation of the EFG due to variation of some physical parameters, such as temperature, pressure, electromagnetic fields, composition, etc., it has in recent years become important to know the actual value of the EFG tensor. The reason is that the state-of-the-art numerical methods for calculation of properties of solids [such as full-potential linear-augmented plane wave[7,8] (FP-LAPW) and full-potential linear-muffin-tin orbital[9] (FP-LMTO)] have now been developed to the point where they yield accurate calculations of EFG's.[10] This fact enables the more direct interpretation of experimental results,[10–13] and the identification of microscopic defects may be facilitated by the comparison of experimental data to theoretical predictions for different candidate structures.[14,15]

The nuclear experimental techniques do not determine directly the EFG but rather one or more characteristic nuclear quadrupole resonance frequencies $\nu_Q$, which are proportional to the EFG and to the nuclear quadrupole moment $Q$ (see Sec. II). Provided an exact value of $Q$ for the nuclear state involved is known, experimental electric field gradient information can be deduced. However, in spite of the wide use of the experimental techniques, for many important probe nuclei the exact $Q$ value is not known with sufficient accuracy. A recent review of the current status is given by Pyykkö.[16] Ideally, theories of the nuclear state should provide values of the nuclear quadrupole moments (see, e.g., Ref. 17), but often the uncertainties involved are larger than what can be accepted for the interpretation of nuclear spectroscopy experiments. Another approach involves the calculation of EFG's by *ab initio* electronic structure methods and comparison with experimental values of NQR frequencies, which is the strategy pursued in Refs. 10–13 and 18 as well as in the present work, and which has led to quite accurate $Q$ values. In this respect it is important that different calculational schemes are compared to prove the validity and consistency of the methods. For example, the solid-state methodology involved in Refs. 10–13 includes the density-functional theory (DFT) and approximations within this scheme, while the quantum-chemical approach of Ref. 18 does not invoke this approximation, and hence is of more fundamental character, but on the other hand restricted to atoms and small molecules.

In the present work the EFG's of several compounds con-

 

taining the elements Cl, Br, and I as constituents are calculated. The nuclear quadrupolar moments for the NQR probes $^{35}$Cl, $^{79}$Br, and $^{127}$I are determined by comparison to experimental NQR frequencies. The solids considered cover a wide range of insulating compounds. For the calculation of the EFG, the electrostatic crystalline potential is determined using state-of-the-art *ab initio* band-theory calculations within DFT.

## II. METHOD

The EFG is a symmetric traceless tensor[4] whose components are defined by the second spatial derivatives of the $\ell=2$ part, $V_{\ell=2}$, of the Coulomb potential at a nuclear position:

$$V_{ij}=\left(\frac{\partial^2}{\partial x_i \partial x_j}-\frac{1}{3}\Delta\right)V_{\ell=2}, \tag{1}$$

where $\Delta$ is the Laplace operator. The Coulomb potential is calculated from the total charge distribution due to electrons and nuclei in the crystal, by solving the Poisson's equation (once the electronic charge distribution has been self-consistently determined). Hence, all shielding and antishielding effects are included in $V_{\ell=2}$.[19] After diagonalization and rearranging the principal components according to $|V_{xx}| \leqslant |V_{yy}| \leqslant |V_{zz}|$, the EFG is by definition given as $V_{zz}$, while the asymmetry parameter

$$\eta \equiv \frac{V_{xx}-V_{yy}}{V_{zz}} \tag{2}$$

specifies the smaller components. The experimental NQR coupling constant $C$ is related to $V_{zz}$ by

$$C=\frac{|eQV_{zz}|}{h}, \tag{3}$$

where $e$ is the electron charge and $h$ is Planck's constant. The Cl and Br NQR isotopes have nuclear spins $I=3/2$, which gives rise to a splitting between the $M=\pm 3/2$ and $M=\pm 1/2$ levels of

$$\nu_Q=\frac{C}{2}\left(1+\frac{1}{3}\eta^2\right)^{1/2}, \tag{4}$$

which is the frequency measured. Hence, it is not possible to determine separately the parameters $C$ and $\eta$ for these isotopes. The $^{127}$I isotope, on the other hand, has nuclear spin $I=5/2$ and a more complex splitting of the nuclear $M$ states into three levels.[2] Therefore, two resonance frequencies can be measured for $^{127}$I and both $C$ and $\eta$ determined. Both $Q$ and $V_{zz}$ can take positive or negative values, but their signs are not determined by the spectroscopy.

For the determination of the electronic structure we used the *ab initio* FP-LAPW method in a scalar relativistic version as implemented in the WIEN2K code.[20] The unit cell is divided into nonoverlapping muffin-tin spheres around the atomic nuclei and the remaining interstitial region, and the corresponding wave functions are expressed as linear combinations of atomiclike functions inside the spheres and plane waves in the interstitial. In addition to the usual LAPW basis set, local orbitals for high-lying core states have been included.[21] No approximation is made for the potential, except for the exchange-correlation potential, for which we in this work have used the generalized gradient approximation (GGA) of Perdew *et al.*[22] The comparison of the local-density approximation (LDA) and GGA for exchange and correlation effects will be discussed for selected cases.

The electronic structure calculations presented here comprise compounds having in their chemical formula one or more of the halide elements Cl, Br, or I. For Cl, we consider solid $Cl_2$, $SbCl_5$, $SbCl_3$, ICl, $ICl_3$, $ClF_3$, and $FeCl_2$. For Br, we consider solid $Br_2$, $CdBr_2$, $\alpha SbBr_3$, $\beta SbBr_3$, $CsBr_3$, and $KBrO_3$. Finally, for I we consider solid $I_2$, $BI_3$, $AsI_3$, $BiI_3$, $CdI_2$, ICl, $ICl_3$, and $SbI_3$. The calculations used the cutoff criterion $R_{\mathrm{mt}}K_{\max}=8$, where $R_{\mathrm{mt}}$ is the smallest muffin-tin radius and $K_{\max}$ is the largest wave number of the basis set,[20] and a self-consistency criterion of $10^{-5}$ Ry on the total energy. The number of $k$ points varied in the range 30–100 in the irreducible part of the Brillouin zone, depending on structure. The experimental crystal structures were used throughout, as specified in Tables I–III, and no theoretical determination of crystal parameters was undertaken. Details of the calculation of the EFG within the FP-LAPW code are described in the works of Schwarz and co-workers.[24,25]

TABLE I. Calculated electric-field gradients $V_{zz}$, asymmetry parameters $\eta$, and NQR frequencies $\nu_Q$ [Eq. (4), using Eq. (7)], together with experimental NQR frequencies, for $^{35}$Cl compounds. The electric-field gradients are in units of $10^{21}$ V/m$^2$ and the NQR frequencies in MHz. For compounds with several inequivalent Cl positions, the theoretical values correspond to the nomenclature of the structural reference, with the assignment of the experimental frequencies tentatively suggested by the present authors.

| | | Theory | | | Experiment |
|---|---|---|---|---|---|
| Compound [a] | Space group | $V_{zz}$ | $\eta$ | $\nu_Q$ | $\nu_Q$ [b] |
| $Cl_2$ | $Cmca$ | 51.48 | 0.31 | 108.1 | 108.494 |
| $FeCl_2$ | $R\bar{3}m$ | −2.14 [c] | 0 | 4.42 | 4.74 [c] |
| $SbCl_3$ [d] (1) | $Pnma$ | 19.30 | 0.18 | 40.1 | 38.612 |
| (2) | | 20.91 | 0.03 | 43.2 | 41.828 |
| $SbCl_5$ (1) | $P6_3/mmc$ | 27.22 | 0 | 56.3 | 55.71 [e] |
| (2) | | 29.08 | 0.22 | 60.6 | 60.36 |
| $ICl_3$ (1) | $P\bar{1}$ | −16.76 | 0.25 | 35.0 | 27.480 (RT) |
| (2) | | 33.26 | 0.16 | 69.0 | 71.360 |
| (3) | | 31.48 | 0.17 | 65.4 | 67.832 |
| $\alpha$ ICl (1) | $P2_1/c$ | 24.92 | 0.59 | 54.4 | [f] |
| (2) | | 37.94 | 0.05 | 78.5 | 74.368 (RT) |
| $ClF_3$ | $Pnma$ | −73.14 | 0.06 | 151.3 | 150.259 |

[a] Experimental crystal structures are from Ref. 23, except where noted.

[b] Experimental NQR frequencies are from Ref. 2. Data refer to low temperature (77 K).

[c] Paramagnetic phase.

[d] Reference 26.

[e] Average of two frequencies reported at 55.56 and 55.86 MHz.

[f] This line has not been observed experimentally.

TABLE II. Calculated electric-field gradients $V_{zz}$, asymmetry parameters $\eta$, and NQR frequencies $\nu_Q$ [Eq. (4) using Eq. (8)], together with experimental NQR frequencies, for $^{79}$Br compounds. Units as in Table I.

| Compound [a] | Space group | Theory $V_{zz}$ | Theory $\eta$ | Theory $\nu_Q$ | Experiment $\nu_Q$ [b] |
|---|---|---|---|---|---|
| $Br_2$ | $Cmca$ | 94.25 | 0.43 | 775 | 765.04 |
| $CdBr_2$ | $R\bar{3}m$ | −3.92 | 0 | 31 | 34.086 |
| $\alpha SbBr_3$ [c] (1) | $P2_12_12_1$ | 40.12 | 0.36 | 327 | 329.484 [e] |
| (2) | | 40.12 | 0.05 | 320 | 327.722 [e] |
| (3) | | 45.09 | 0.10 | 360 | 343.190 [e] |
| $\beta SbBr_3$ [d] (1) | $Pbnm$ | 43.38 | 0.18 | 348 | 329.020 [e] |
| (2) | | 44.30 | 0.03 | 353 | 345.925 [e] |
| $KBrO_3$ | $R3m$ | −44.86 | 0 | 358 | 357.600 |
| $CsBr_3$ [f] (1) | $Pmnb$ | 33.66 | 0.33 | 273 | [g] |
| (2) | | 101.81 | 0.15 | 815 | 814.00 (RT) |
| (3) | | 63.71 | 0.15 | 510 | 503.40 (RT) |

[a]Experimental crystal structures are from Ref. 23, except where noted.
[b]Experimental NQR frequencies are from Ref. 2, except where noted. Data refer to low temperature (77 K), except where noted.
[c]Reference 27.
[d]Reference 28.
[e]Reference 29.
[f]Reference 30.
[g]This line has not been observed experimentally.

Both Cl and Br possess two naturally occurring NQR isotopes, $^{35}$Cl and $^{37}$Cl, and $^{79}$Br and $^{81}$Br, respectively, while I has only the $^{127}$I isotope. From comparison of frequencies in the same solid, the ratios of nuclear quadrupole moments are well established:[2]

$$\frac{Q(^{35}\mathrm{Cl})}{Q(^{37}\mathrm{Cl})} = -1.2688 \tag{5}$$

and

$$\frac{Q(^{79}\mathrm{Br})}{Q(^{81}\mathrm{Br})} = +1.197\,07. \tag{6}$$

In the following we will only consider experimental results obtained for $^{35}$Cl, $^{79}$Br, and $^{127}$I.

### III. RESULTS

Tables I–III summarize the EFG's calculated in the present work, together with available experimental NQR data. In most cases, experiments are done at low temperature (77 K or below), but a few compounds have only been measured at room temperature. Under usual circumstances, NQR frequencies shift down with temperature, of the order of 1% between 0 and 300 K.[2,32] No temperature correction was included in the experimental data. The calculations always refer to 0 K.

Figures 1–3 display the plots of the data from the tables, and the best linear fits are shown. For $^{35}$Cl and $^{79}$Br the experimental frequency $\nu_Q$ is plotted versus the calculated combination $|V_{zz}|(1+\eta^2/3)^{1/2}$, in order to investigate the relation (4). For $^{127}$I, we plot the coupling constant $C$ versus the calculated EFG to validate the relation (3). From the best linear fits in the figures, the nuclear quadrupole moments are obtained as

TABLE III. Calculated electric-field gradients $V_{zz}$, asymmetry parameters $\eta$, and nuclear quadrupole coupling constant $C$ [Eq. (3) using Eq. (9)], together with experimental nuclear quadrupole coupling constants and asymmetry parameters for $^{127}$I compounds. Units as in Table I. For $\alpha$ ICl, the two inequivalent I positions correspond to the nomenclature of Ref. 23.

| Compound [a] | Space group | Theory $V_{zz}$ | Theory $\eta$ | Theory $C$ | Experiment $\eta$ [b] | Experiment $C$ [b] |
|---|---|---|---|---|---|---|
| $I_2$ | $Cmca$ | 114.32 | 0.57 | 1993 | 0.173 | 2157.18 |
| $BI_3$ | $P6_3$ | 69.37 | 0.53 | 1209 | 0.455 | 1242.4 |
| $AsI_3$ [c] | $R\bar{3}$ | 76.28 | 0.25 | 1330 | 0.1891 | 1330.23 |
| $SbI_3$ [c] | $R\bar{3}$ | 51.50 | 0.72 | 898 | 0.565 | 895.83 |
| $BiI_3$ [c] | $R\bar{3}$ | −42.48 | 0.20 | 740 | 0.290 | 682.18 |
| $CdI_2$ | $P\bar{3}m1$ | −5.84 | 0 | 102 | 0.028 | 98.27 |
| $ICl_3$ | $P\bar{1}$ | −178.73 | 0.18 | 3116 | 0.0772 | 3034.9 |
| $\alpha$ ICl (1) | $P2_1/c$ | 174.29 | 0.05 | 3038 | 0.0298 | 3046.4 |
| (2) | | 150.37 | 0.52 | 2621 | | |

[a]Experimental crystal structures are from Ref. 23, except where noted.
[b]Experimental NQR frequencies and $\eta$ values are from Ref. 2. Data refer to low temperature (77 K).
[c]Reference 31.

$$|Q(^{35}\mathrm{Cl})| = 0.0855 \pm 0.0011 \text{ b}, \tag{7}$$

$$|Q(^{79}\mathrm{Br})| = 0.330 \pm 0.005 \text{ b} \tag{8}$$

and

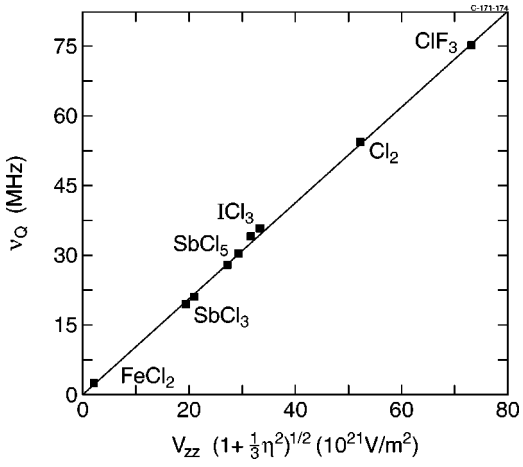


FIG. 1. Experimental NQR frequencies vs calculated $|V_{zz}|(1+\eta^2/3)^{1/2}$ for $^{35}$Cl compounds. Units as in Table I. The straight line is the best linear fit.

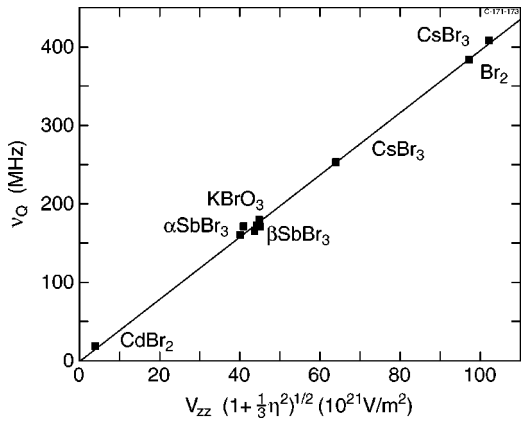


FIG. 2. Same as Fig. 1 but for $^{79}$Br compounds. Units as in Table II. The straight line is the best linear fit.

$$|Q(^{127}\mathrm{I})| = 0.721 \pm 0.026 \ \ \mathrm{b}. \tag{9}$$

With the ratios, Eqs. (5) and (6), we further derive

$$|Q(^{37}\mathrm{Cl})| = 0.0673 \pm 0.0009 \ \ \mathrm{b} \tag{10}$$

and

$$|Q(^{81}\mathrm{Br})| = 0.276 \pm 0.004 \ \ \mathrm{b}. \tag{11}$$

The signs of the nuclear quadrupole moments are not determined. From other spectroscopies,[2] it is known that $^{35}$Cl and $^{127}$I have a negative quadrupole moment, while the other nuclei have positive $Q$ values.

The figures reveal excellent linear relationships between the calculated EFG's and the experimental NQR data. The remaining small fluctuations can have their origin both in the experimental and in the numerical uncertainties. Experimental difficulties arise from the quality of the samples and the accuracy of the determination of the crystal structures. On the theoretical side, the validity of the GGA is assumed, and spin-orbit and temperature effects are neglected (all calculations are for $T=0$). The quoted error bars on the nuclear quadrupole moments in Eqs. (7)–(11) reflect the purely statistical spread of the experimental and theoretical data, while we have no estimates of possible systematic error bars. The wide range of NQR frequencies considered in this work minimize these statistical uncertainties.

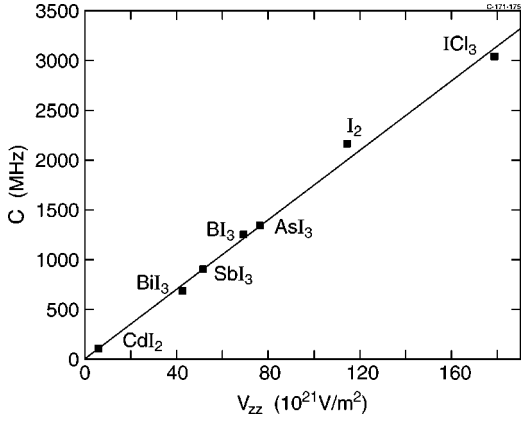


FIG. 3. Calculated EFG (absolute value) vs experimental NQR coupling constant $C$, Eq. (3), for $^{127}$I compounds. Units as in Table III. The straight line is the best linear fit.

## IV. DISCUSSION

The results obtained for Br and I, Eqs. (8) and (9), may be compared with the values obtained by Bieroń *et al.*,[18] who determined $Q(^{79}\mathrm{Br}) = 0.313 \pm 0.003$ b and $Q(^{127}\mathrm{I}) = -0.710 \pm 0.010$ b, using a numerically accurate molecular method (configuration-interaction quantum-chemical calculations using Gaussian orbitals). It is reassuring for both theoretical approaches that the derived quadrupole moments are so close. In particular, the GGA approximation applied in the present solid-state calculations is proven to be valid also for the calculation of a sensitive quantity such as the EFG. Our results confirm the assertion by Bieroń *et al.*[18] that the value of $Q(^{127}\mathrm{I}) = -0.789$ b, accepted until recently, should be slightly revised.[16] For Br, our result coincides with the value accepted prior to the work of Bieroń *et al.*, $Q(^{79}\mathrm{Br}) = 0.331$ b,[16] which is 7% larger than the value given in Ref. 18.

For Cl, similar highly accurate quantum-chemical calculations[33] for the Cl atom led to the value $Q(^{35}\mathrm{Cl}) = -0.081\,65 \pm 0.0008$ b, again in very fine agreement with the value obtained here from the solid-state systems. Surprisingly, the value hitherto accepted[16] for $^{35}$Cl, $Q(^{35}\mathrm{Cl}) = -0.08249 \pm 0.00002$, obtained by Sternheimer[34] by estimating atomic shielding and antishielding factors, is also in excellent agreement with the present value, Eq. (6), as well as that of Ref. 33.

There are several comments to make to the data presented in Tables I–III. For ICl, two crystalline forms exist, $\alpha$ ICl and $\beta$ ICl, which both possess two inequivalent crystallographic positions for both I and Cl. Only the $\alpha$ ICl structure was considered here, for which we have found two quite distinct values of the EFG for both constituents. Experimentally, only one frequency is reported, both for $^{35}$Cl and $^{127}$I, which is puzzling. The available $^{35}$Cl data are quite similar in the $\alpha$ ICl and $\beta$ ICl structure. One extra broad feature is seen in the spectra of $^{127}$I, which has not been identified, though.[35] The observed frequency is tentatively associated with one of the calculated EFG's for both Cl and I in Tables I and III. Due to this lack of experimental completeness we have left ICl out of the analysis in Figs. 1 and 3. Similarly, for $CsBr_3$, the three crystallographic Br positions each have their distinct EFG, while experimentally only two frequencies are observed. The two larger frequencies are in nice agreement with the experimental values. Presumably the low frequencies were not scanned in the experiment. In this case, the two larger frequencies were included in the fit in Fig. 2. For $FeCl_2$, the calculations assumed a paramagnetic phase, as the experimental data were taken at temperatures above the ordering Néel temperature.

The Sb compounds were also investigated in a similar study in Ref. 12, based upon the FP-LMTO method, and concordance was indeed found between the Sb and halide EFG's as calculated with this method and with the FP-LAPW method applied in the present study (see Table IV).

TABLE IV. Calculated electric-field gradients $V_{zz}$ in units of $10^{21}$ V/m$^2$, and asymmetry parameters $\eta$ for ligands of halide compounds. Where available, comparison to other work is given.

| Atom | Compound | Theory $V_{zz}$ | Theory $\eta$ | Other work $V_{zz}$ |
|---|---|---|---|---|
| Sb | $\alpha SbBr_3$ | −21.00 | 0.18 | −18.23, [a] −19.53 [b] |
| Sb | $\beta SbBr_3$ | −21.53 | 0.21 | −19.02, [a] −21.28 [b] |
| Sb | $SbI_3$ | −4.63 | 0 | −2.62, [a] −5.24 [b] |
| Sb | $SbCl_5$ | −5.00 | 0 | −4.99, [a] −5.24 [b] |
| Sb | $SbCl_3$ | −29.55 | 0.03 | 22.96, [a] −23.73 [b] |
| Cd | $CdI_3$ | 0.24 | 0 | 0.43 [c] |
| Cd | $CdBr_3$ | 0.85 | 0 | 1.10 [c] |
| As | $AsI_3$ | −5.69 | 0 | −7.73 [d] |
| Fe | $FeCl_2$ | 0.90 [e] | 0 | |
| F(1) | $ClF_3$ | 40.29 | 0.03 | |
| F(2) | $ClF_3$ | 25.61 | 0.20 | |
| Bi | $BiI_3$ | −0.09 | 0 | |
| K | $KBrO_3$ | 0.41 | 0 | |
| O | $KBrO_3$ | 19.33 | 0.57 | |
| Cs | $CsBr_3$ | −21.15 | 0.48 | |
| B | $BI_3$ | 2.14 | 0 | |

[a]Theoretical value using the FP-LMTO method and LDA, Ref. 12.
[b]Experimental value from Ref. 2, using the theoretical sign and Sb nuclear quadrupole moment determined in Ref. 12.
[c]Experimental value, Ref. 40, using $Q(\mathrm{Cd}) = 0.78$ b, as recommended by Ref. 16. Sign is assumed positive.
[d]Experimental value, Ref. 2, using $Q(\mathrm{As}) = 0.314$ b, as recommended by Ref. 16. Sign is assumed negative.
[e]Paramagnetic phase.

For $SbCl_5$ three $^{35}$Cl frequencies were observed, while the crystal structure only leads to two distinct Cl positions.[23] The two lower frequencies are, however, rather close, for which reason we have associated them with the same crystallographic position. The observed signal-to-noise ratio suggests an occurrence of 1:1:3 of the corresponding Cl specimens, with the first two being those associated with the close lower frequencies. The two crystallographic Cl atoms occur in the ratio 2:3, which then also supports this assignment. We have no explanation for the possible origin of the splitting of this line.

The theoretical data in Tables I–III include the calculated asymmetry parameter $\eta$ and the EFG sign. Experimentally, the $\eta$ parameter can be extracted from NQR spectroscopy only for $^{127}$I, for which reason Table III includes this information. The agreement is reasonably good, with exception of solid $I_2$, where the calculated $\eta$ is 0.57, while the experimental value is only 0.17. We have no explanation for this fact. It is striking that apart from $BiI_3$ and $CdI_2$, the calculated $\eta$ is always larger than the experimental one. For $CdI_2$, the structure dictates a vanishing $\eta$ parameter, while a small experimental value is reported, which could be due to small heterogeneities. The sign of $QV_{zz}$ for $^{127}$I can be derived from Mössbauer spectroscopy,[36] revealing a negative EFG in $ICl_3$ and a positive one in $I_2$ and ICl [given a negative $Q(^{127}\mathrm{I})$], which agree with the signs found for these compounds in the present calculations.

In Table IV we list the calculated EFG for the nonhalide ligands of the compounds discussed in Tables I–III, together with available theoretical and experimental information from previous work. The agreement is good, but not perfect. For the Sb compounds the two calculations give EFG's of about equal accuracy compared to experiment. Note that the FP-LMTO calculations of Ref. 12 used the LDA, while the present FP-LAPW calculations have used the GGA for exchange-correlation effects. We have further tested, within the FP-LAPW method, the importance of using either the GGA or the LDA for the cases of $Cl_2$, $Br_2$, and $I_2$. The EFG calculated with LDA are $53.81\times10^{21}$ V/m$^2$, $99.28\times10^{21}$ V/m$^2$, and $121.40\times10^{21}$ V/m$^2$, respectively, which represent fluctuations of the order of 5% with respect to the corresponding values calculated with the GGA, cf. Tables I–III. Variations of similar magnitude were also seen for EFG's calculated in wurtzite GaN (Ref. 37) and for small Fe molecules.[38] The influence of other approximate functionals on hyperfine parameters, including hybrids with exact exchange, was investigated in Refs. 38 and 39, in this case showing larger fluctuations in calculated EFG's between different approximation schemes.

Schwerdtfeger *et al.*[38] also compared several DFT-based methods with *ab initio* quantum-chemical calculations for small molecules containing Fe, and concluded that the DFT-based schemes may cause errors for transition-element compounds. On the other hand, it appears that in the quantum-chemical calculations of Ref. 38, it had not been possible to achieve sufficient convergence with respect to basis set. Similar problems do not occur for the DFT-based methods, which use complete basis sets.

## V. SUMMARY

The nuclear quadrupole moment for the halide isotopes $^{35}$Cl, $^{37}$Cl, $^{79}$Br, $^{81}$Br, and $^{127}$I were determined by comparison of experimental values for the nuclear quadrupole frequencies to *ab initio* calculated EFG's at the halide site in several compounds. The nuclear quadrupole moments derived compare favorably with values recently obtained by independent quantum-chemical methods applied to atoms and small molecules. From the present work, it is suggested that the generally accepted value for the nuclear quadrupole moment of $^{127}$I should be slightly corrected.

## ACKNOWLEDGMENTS

The authors thank Dr. G. Etcheverría for his collaboration and his help with many crystallographic structures. This work was partially supported by CONICET.

[1] D. Canet, *Nuclear Magnetic Resonance: Concepts and Methods* (Wiley, Chichester, 1996).
[2] G.K. Semin, T.A. Babushkina, and G.G. Yakobson, *Nuclear Quadrupole Resonance in Chemistry* (Wiley, New York, 1975).
[3] H. Frauenfelder and R.M. Steffen, in *Alpha-, Beta-, and Gamma-Ray Spectroscopy*, edited by K. Siegbahn (North-Holland, Amsterdam, 1968), Vol. 2, p. 997.
[4] N.N. Greenwood and T.C. Gibb, *Mössbauer Spectroscopy* (Chapman and Hall, London, 1971).
[5] *Mössbauer Spectroscopy*, edited by U. Gonser (Springer, Berlin, 1975).
[6] J.A. Weil, J.R. Bolton, and J.A. Wertz, *Electron Paramagnetic Resonance: Elementary Theory and Practical Applications* (Wiley, New York, 1994).
[7] O.K. Andersen, Phys. Rev. B **12**, 3060 (1975).
[8] D.D. Koelling and G.O. Arbman, J. Phys. F: Met. Phys. **5**, 2041 (1975).
[9] M. Methfessel, Phys. Rev. B **38**, 1537 (1988); M. Methfessel, C.O. Rodriguez, and O.K. Andersen, *ibid.* **40**, 2009 (1989).
[10] P. Dufek, P. Blaha, and K. Schwarz, Phys. Rev. Lett. **75**, 3545 (1995).
[11] A. Svane, N.E. Christensen, C.O. Rodriguez, and M. Methfessel, Phys. Rev. B **55**, 12 572 (1997); A. Svane, L. Petit, W.M. Temmerman, and Z. Szotek, *ibid.* **66**, 085110 (2002).
[12] A. Svane, Phys. Rev. B **68**, 064422 (2003).
[13] P.E. Lippens, Phys. Rev. B **60**, 4576 (1999).
[14] P. Blaha, K. Schwarz, W. Faber, and J. Luitz, Hyperfine Interact. **126**, 389 (2000).
[15] M. Fanciulli, A. Zenkevich, I. Wenneker, A. Svane, N.E. Christensen, and G. Weyer, Phys. Rev. B **54**, 15 985 (1996); M. Fanciulli, C. Rosenblad, G. Weyer, A. Svane, N.E. Christensen, and H. von Känel, J. Phys.: Condens. Matter **9**, 1619 (1997); M. Fanciulli, G. Weyer, A. Svane, N.E. Christensen, H. von Känel, E. Müller, N. Onda, L. Miglio, F. Tavazza, and M. Celino, Phys. Rev. B **59**, 3675 (1999); M. Corti, A. Gabetta, M. Fanciulli, A. Svane, and N.E. Christensen, *ibid.* **67**, 064416 (2003).
[16] P. Pyykkö, Mol. Phys. **99**, 1617 (2001).
[17] G. Martínez-Pinedo, P. Schwerdtfeger, E. Caurier, K. Langanke, W. Nazarewicz, and T. Söhnel, Phys. Rev. Lett. **87**, 062701 (2001).
[18] J. Bieroń, P. Pyykkö, D. Sundholm, V. Kellö, and A.J. Sadlej, Phys. Rev. A **64**, 052507 (2001).
[19] J. Ehmann and M. Fähnle, Phys. Rev. B **55**, 7478 (1997).
[20] P. Blaha, K. Schwarz, G.K.H. Madsen, D. Kvasnicka, and J. Luitz, *WIEN2k, An Augmented Plan Wave + Local Orbitals Program for Calculating Crystal Properties* (Karlheinz Schwarz, Technical University, Vienna, Austria, 2001).
[21] D. Singh, Phys. Rev. B **43**, 6388 (1991).
[22] J.P. Perdew, K. Burke, and M. Ernzerhof, Phys. Rev. Lett. **77**, 3865 (1996).
[23] R.W.G. Wyckoff, *Crystal Structures* (Plenum Press, New York, 1972), Vols. 1 and 2.
[24] K. Schwarz, C. Ambrosch-Draxl, and P. Blaha, Phys. Rev. B **42**, 2051 (1990).
[25] K. Schwarz and P. Blaha, Z. Naturforsch., A: Phys. Sci. **47**, 197 (1992).
[26] A. Lipka, Acta Crystallogr., Sect. B: Struct. Crystallogr. Cryst. Chem. **35**, 3020 (1979).
[27] D.W. Cushen and R. Hulme, J. Chem. Soc. **1964**, 4162.
[28] D.W. Cushen and R. Hulme, J. Chem. Soc. **1962**, 2218.
[29] G.L. Brenemann and R.D. Willett, Acta Crystallogr., Sect. B: Struct. Crystallogr. Cryst. Chem. **B25**, 1073 (1969).
[30] H. Negita, T. Okuda, and M. Kashima, J. Chem. Phys. **45**, 1076 (1966).
[31] J. Trotter and T. Zobel, Z. Kristallogr. **123**, 67 (1966).
[32] Temperature effects on the EFG can become substantial in cases, where temperature induces significant changes to structural parameters, or where significant redistribution of electronic charge occurs, such as, e.g., in narrow-gap semiconductors [N.E. Christensen, I. Wenneker, A. Svane, and M. Fanciulli, Phys. Status Solidi B **198**, 23 (1996)].
[33] D. Sundholm and J. Olsen, J. Chem. Phys. **98**, 7152 (1993).
[34] R.M. Sternheimer, Phys. Rev. A **6**, 1702 (1972).
[35] S. Kojima, K. Tsukada, S. Ogawa, and A. Shimauchi, J. Chem. Phys. **23**, 1963 (1955).
[36] M. Pasternak and T. Sonnino, J. Chem. Phys. **48**, 1997 (1968).
[37] N.E. Christensen (unpublished).
[38] P. Schwerdtfeger, T. Söhnel, M. Pernpointner, J.K. Laerdahl, and F.E. Wagner, J. Chem. Phys. **115**, 5913 (2001).
[39] O.Kh. Poleshchuk, J.N. Latosińska, and V.G. Yakimov, Phys. Chem. Chem. Phys. **2**, 1877 (2000).
[40] H. Haas and D.A. Shirley, J. Chem. Phys. **58**, 3339 (1973).